

# **On the response of flax fiber reinforced composites under salt-fog/dry conditions: reversible and irreversible performances degradation**

**V. Fiore\*<sup>1</sup>, L. Calabrese<sup>2</sup>, R. Miranda<sup>1</sup>, D. Badagliacco<sup>1</sup>, C. Sanfilippo<sup>1</sup>, D. Palamara<sup>2</sup>, A.  
Valenza<sup>1</sup>, E. Proverbio<sup>2</sup>**

<sup>1</sup>Department of Engineering, University of Palermo

Viale delle Scienze, Edificio 6, 90128 Palermo, Italy

Email: [vincenzo.fiore@unipa.it](mailto:vincenzo.fiore@unipa.it)

<sup>2</sup>Department of Engineering, University of Messina

Contrada Di Dio (Sant'Agata), 98166 Messina, Italy

\*Corresponding Author

## Abstract

Despite their scarce resistance to humid or wet conditions, natural fiber reinforced composites (NFRCs) seem to be able to partially recover their performances under discontinuous exposition to marine environment. To investigate this peculiarity, flax fiber reinforced composite was at first subjected to salt-fog spray condition at 35 °C for 15 and 30 days, respectively, and then stored in “dry” condition (i.e., 50% R.H. and 22°C) between 0 and 21 days. The performances evolution was evaluated through flexural tests, water uptake and contact angle measurements. Moreover, the morphology of fractured mechanical samples was examined by using 3D optical microscope and scanning electron microscope (SEM).

Flax fiber reinforced composite experienced phenomena of both reversible and irreversible degradation during the wet phase thus evidencing a relevant mechanical recovery thanks to the drying. Quite interestingly, the laminate showed an almost complete recovery of the flexural strength, meaning that this property is more strictly related to mainly reversible aging phenomena whereas the greater stiffness loss is more probably due to irreversible ones.

**Keywords:** A. Polymer-matrix composites (PMCs); B. Environmental degradation; D. Mechanical testing; Moisture desorption

## 1 Introduction

It is widely known that an increasing attention was paid in the last decades to Natural Fiber Reinforced Composites (NFRCs) due to their good features such as recyclability, eco-compatibility, health advantages, lightweight, good processability, large availability and cost-effectiveness. Among natural or plant fibers, flax is widely used as reinforcement for composite materials thanks to its large availability and high specific mechanical properties, comparable to those of glass fibers [1].

Nevertheless, due to some design constraints, the use of natural fibers is mainly limited in several engineering fields to non-structural or semi-structural applications. One of the major drawbacks consists in their lower and highly variable mechanical properties in comparison to their synthetic counterparts (i.e., glass, Kevlar and carbon fibers). Another aspect hindering further implementation of NFRCs is their scarce aging resistance when subjected to humid environmental conditions [2–4]. This can be ascribed to the hydrophilic behavior of natural fibers that, due to their polysaccharide components (i.e., mainly pectin, cellulose and hemicellulose) having strongly polarized hydroxyl groups, tend to absorb large amounts of moisture [5]. Hence, natural fibers easily soften and swell with absorbed water molecules, which could negatively affect the mechanical performances of NFRCs [6]. Furthermore, this leads to poor adhesion with several hydrophobic polymeric matrices, thus further decreasing the mechanical response of NFRC materials [7].

In order to cope with these issues, several authors showed that the hybridization of natural fibers with synthetic ones represents a valid tool [8–15]. Another approach aimed to improve the moisture resistance of NFRC components, thus extending their service life in humid environmental conditions, can be represented by chemical or physical treatments of natural fibers [16–21].

A wide literature is available on the evaluation and prediction of the behavior of natural fibers and their composites after a continuous exposition to humid or wet environments or after wet/dry aging cycles. Nevertheless, relatively few studies have been focused on the understanding of how these aged materials can recover their performances after a dry phase.

Ventura et al. [22] showed the effects of a wet/dry cycling on flax nonwoven fabrics to stabilize the cellulosic fibers against humidity changes thus achieving greater stability against the water absorption. The impact of wet/dry cycles (i.e., 3.5 days at 90% HR and 3.5 days at 40% HR, both at 55 °C) on the longitudinal tensile properties of a unidirectional flax/epoxy composite was investigated by Cadu et al. [23]. This material showed moderate decreases in the mechanical performance (i.e., about -10% of the moduli and about -14% of the ultimate tensile stress) after 1 year of exposure and 52 cycles of aging. In another paper of the authors [24], they evaluated the effect of the same aging conditions on the composite transverse mechanical properties, showing noticeable decrements in both transverse tensile strength (i.e., about -20% after the first week of ageing) and modulus (i.e., about -18% already after the first week to reach about -45% after 1 year). These results were mainly ascribed to the plasticization of the epoxy matrix.

Hence, the academia focused its attention in last years on the assessment of performances modification and damage development of flax fiber reinforced composites when subjected to cycling hydrothermal or wet/dry aging, indicating that the topic is acquiring relevant interest in natural fiber composite durability design. Nevertheless, at the best of our knowledge, no paper assessed the behavior of flax fiber reinforced composites under alternated salt-fog exposition and dry phases, showing how this kind of materials can recover their performances due to the latter phase.

In this context, the present paper is addressed to investigate the modification of the mechanical performances and related fracture mechanisms of flax fiber reinforced composites under salt-fog/dry conditions. In particular, woven flax fabric reinforced epoxy composite was at first subjected to salt-fog spray condition at 35 °C for 15 and 30 days, respectively. Afterwards, a dry stage (i.e., 50% R.H. and 22°C) for a time varying between 0 and 21 days was carried out. Quasi-static flexural tests, water uptake and water contact angle measurements were performed on both unaged and aged samples. Moreover, the surface morphology of fractured surfaces after flexural testing was examined by using 3D optical microscope and scanning electron microscope (SEM).

## 2 Experimental

### 2.1 Materials and Methods

Flax fiber reinforced polymer square panels (30 cm x 30 cm x 0.335 cm) were manufactured via vacuum assisted resin infusion process by using a two-stage vacuum pump model VE 235 D by Eurovacuum, The Netherlands. In particular, each panel was cured at 25 °C for 24 h and post-cured at 50 °C for 15 h.

A DEGBA epoxy resin (SX8 EVO by Mates Italiana s.r.l., Italy) mixed with its own amine-based hardener (100:30 by weight) and five flax balanced twill weave woven fabrics having nominal areal weight of 318 g/m<sup>2</sup> (Lineo, France) were used as matrix and reinforcement of the composites, respectively.

### 2.2 Salt-fog/dry aging phases

The goal of this paper is the assessment of the effect of the dry phase on the capability of NFRCs to recover their mechanical performances after aging in wet environmental conditions such as marine one.

To this aim, composite panels were subjected to salt-fog spray condition (i.e., 5 wt.% NaCl solution) at a constant temperature of 35 °C, by using a climatic chamber model SC/KWT 450 (Weiss, Germany), in accordance with ASTM B 117 standard (in the next “wet phase”). At the end of this phase, five specimens for each investigated condition were cut to their nominal dimensions (i.e., depending on the specific test) by using a diamond blade saw. Afterwards, the aged specimens were stored in “dry” condition (i.e., 50% relative humidity and 22 °C temperature) before carrying out the mechanical tests (in the next “dry phase”)

For sake of clearness, specimens will be named with a “WxDy” code, where x and y indicate the time intervals, expressed in days, of the “wet” (i.e., salt-fog spray conditions) and “dry” phases,

respectively. For instance, W15D1 indicates specimens exposed to salt-fog environment for 15 days and then dried for 1 day. Similarly, W0D0 indicates unaged specimens (i.e., reference).

### 2.3 Water uptake

In order to evaluate the water uptake trend at increasing the exposure time to salt-fog according to ASTM D570 standard, three square samples (100 mm × 100 mm) were periodically removed from the salt-fog chamber within the range 1–30 days, cleaned with a dry cloth and weighed by using an analytical balance (model AX 224 by Sartorius, Germany) with precision 0.1 mg. The water uptake (WU, in percentage) of NFRCs was calculated according to the following equation:

$$WU(\%) = \frac{W_{ti} - W_0}{W_0} \cdot 100 \quad \text{Eq. 1}$$

Where  $W_0$  and  $W_{ti}$  are the weight of the dry unaged and aged at  $t_i$  exposure time in salt fog chamber, respectively.

Further analysis of water absorption and desorption characteristics of flax fiber reinforced composites was performed by measuring the diffusion coefficient  $D$ . In particular, this parameter was determined as the slope of the water uptake versus the square root of the time curve, according to the following equation:

$$D = \pi \left( \frac{h}{4M_\infty} \right)^2 \left( \frac{M_2 - M_1}{\sqrt{t_2} - \sqrt{t_1}} \right)^2 \quad \text{Eq. 2}$$

where  $M_\infty$  is the water uptake at saturation,  $h$  is the thickness of the specimen (expressed in mm),  $\frac{M_2 - M_1}{\sqrt{t_2} - \sqrt{t_1}}$  is the slope of the curve in the time range ( $t_2 - t_1$ ), expressed in s, considering that in the initial stage of the process the absorption/desorption phenomenon is linear.

At the end of the wet phase, the mass of W15 and W30 samples (i.e., exposed to salt-fog condition for 15 and 30 days, respectively) was monitored even during the dry phase to evaluate the mass recovery capability of NFRCs when subjected to drying at controlled conditions.

## 2.4 Morphological analysis

The fractured surfaces of flexural specimens were analyzed by 3D optical microscope (model KH8700 3D digital microscope by Hirox, Japan) and Scanning Electron Microscope (SEM - model XL30 ESEM by Philips microscope, The Netherlands) operating at 10 kV. Prior to SEM analysis, each sample was sputter-coated with a thin layer of gold to avoid electrostatic charging under the electron beam and rubbed upon a 25 mm diameter aluminum disc.

## 2.5 Density and void content measurements

During the water uptake test, density measurements were carried out on W15 and W30 batches. The experimental density of the composites ( $\rho_{ce}$ ) was determined through a helium pycnometer (model Pycnomatic ATC by Thermo Electron Corporation, US) and the same analytical balance used for the water uptake monitoring. For each sample, 10 measures were carried out and average values were recorded. All the measured standard deviations were lower than 0.01 g/cm<sup>3</sup>.

On the other hand, the theoretical density of the composites ( $\rho_{ct}$ ) was calculated, applying the mixture rule, by using the following equation:

$$\rho_{ct} = \frac{1}{\sum_{i=1}^n W_i / \rho_i} \quad \text{Eq. 3}$$

Where,  $W$  and  $\rho$  indicate the weight fraction and density, respectively, whereas the subscript  $i$  is referred to the composite constituents (i.e., fiber and matrix). By comparing the experimental and theoretical density values, the volume fraction of voids ( $V_V$ ) can be determined, according to ASTM D2734 standard, by using the following equation:

$$V_V = \frac{\rho_{ct} - \rho_{ce}}{\rho_{ct}} \quad \text{Eq. 4}$$

## 2.6 Wettability measurements

The static water contact angle (WCA) of the composite laminates was measured using an Attension Theta Tensiometer instrument (Attension, Biolin Scientific, Sweden), by applying the sessile drop technique. In detail, a droplet (i.e., 3  $\mu\text{L}$ ) of distilled water was placed on the sample surface and a micro-CCD camera recorded the droplet profile and determined the contact angle measurements with the aid of a suitable PC Attension software (OneAttension V. 2.3). All the measurements were performed open to air at room temperature (i.e., 25  $^{\circ}\text{C}$ ). For each sample, ten water contact angle measurements, homogeneously distributed on the surface, were carried out and average values were recorded. For wetted samples, the surface has been dried with a dry cloth before to perform contact angle measurements.

## 2.7 Quasi-static mechanical tests

Quasi-static three-point bending tests were performed in accordance with ASTM D790 standard. Five specimens (13 mm x 64 mm) for each investigated condition were tested by using a U.T.M. model Z005 (Zwick-Roell, Germany), equipped with 5 kN load cell. The support span and crosshead speed were set equal to 54 mm and 1.4 mm/min, respectively.

# 3 Results and discussion

## 3.1 Water absorption/desorption

Figure 1 shows the weight variation, due to absorption and desorption in wet and dry phases, at increasing aging time (expressed in hours) for all composite batches.

A progressive water uptake by increasing the exposition time can be observed during the wet phase (i.e., salt-fog exposition). For short salt-fog exposition times (i.e., W15 batch), the water uptake curve exhibits a high slope ( $\Delta\text{WU}/\Delta t$ ), reaching a weight gain above 5% already after 7 aging days (i.e., 168 hours). Afterwards, a gradual deflection of the weight gain trend takes place at longer times. In



particular, composites (i.e., W30 batch) reached a maximum water uptake of 10.6% after 30 days of salt-fog exposition time (i.e., 720 hours). Hence, the wet phase is characterized by a bimodal trend with a knee at about 150 h. This behavior is attributable to various mechanisms that contribute to the increase in water absorption of flax fiber reinforced composites. Preliminary, the hydrophilic nature of the composite constituents plays a relevant role on the water adsorption on its surface supporting the water uptake triggering. The water molecules can interact with the unreacted hydrophilic and polar groups of the epoxy resin such as hydroxyl or amine, thus favoring the formation of preferential paths for the water diffusion [25,26]. At the same time, the marked hydrophilic nature of flax fibers plays an important role in activating and kinetically stimulating the water sorption phenomena in wet or moisture environments [6]. The absorption of water during aging is mainly supported by three main steps [27,28]: at first, defects on the matrix surface are generated with subsequent water diffusion along these micro gaps and pores. Subsequently, the water diffusion is exalted by capillary diffusion at the fiber/matrix interface. Finally, the absorption of water inside the composite stimulates a local detachment of the fiber-matrix interface [5] and the formation of micro-cracks in the matrix itself due to aging phenomena, such as fiber swelling or matrix softening [28]. Furthermore, water molecules can be absorbed by flax fibers leading to the break of the secondary bonds among cellulose macromolecules, thus damaging the fiber and creating new volumes available for further water permeation [29].

These processes, having slow kinetics (i.e., longer activation times), can be responsible for the weight gain in the second water adsorption step (characterized by a lower slope). This is in agreement with the curve trend, which shows a saturation only after about 30 days of salt-fog exposition. This behavior could be ascribed to the aging phenomena that favored an irreversible damage which evolves with time and water uptake, thus leading to a deviation from the Fickian behavior [30].

The curve trend in the dry phase differs depending on the composite batch. W15Dx and W30Dx batches indicate composite laminates exposed to salt-fog for 15 and 30 days, respectively, and then stored in “dry” condition for x days (i.e., drying time). In particular, W15Dx shows a relevant

decrease of weight gain that progressively stabilize, at longer drying time, to a water uptake equal to 1.85%. At the same time, W30Dx (characterized by a WU about 30% higher than W15Dx at the end of the wet phase) exhibits a significant weight loss already during the early hours of the dry phase. A reduction of about 4.5 % of the water uptake takes place in the first 24 hours (showing a weight loss from 10.53% to 6.01%). Finally, a plateau can be observed at longer drying time (i.e., WU ~ 2.63%). This behavior indicates that a large part of the water absorbed during the wet phase can be easily released during the dry phase. However, a local degradation of the composite that can be defined as permanent, can be considered taking into account the residual weight gain shown even after long drying times.

In order to have further insights on the ability of water molecules to penetrate inside the composites, the diffusion coefficient  $D$  was determined during sorption and desorption process through Eq. 2 by evaluating the slope of the water uptake versus the square root of time plot, calculated based on (Figure 2).

The initial slope of the curve (red dotted line in Figure 2) was used to determine the diffusion coefficient. The absorption of water during the salt spray fog exposition (Figure 2a) is characterized by a  $D$  value equal to  $7.73 \cdot 10^{-7}$  mm<sup>2</sup>/s. It is almost two orders of magnitude lower than desorption process occurred during the drying. In fact, the diffusion coefficient values during the desorption phenomenon were equal to  $4.22 \cdot 10^{-5}$  mm<sup>2</sup>/s and to  $5.01 \cdot 10^{-5}$  mm<sup>2</sup>/s for W15Dx and W30Dx batches, respectively. These different values indicate that the weight gain of the composite laminate is the kinetic limiting factor in the proposed aging cycle. During the dry phase, samples showed a fast weight loss only in the early drying days. In more detail, this behavior is much faster for the sample exposed to salt-fog for longer time (i.e., W30Dx). The faster dehydration phase can be ascribed to the microstructural modification in the composite laminate due to the formation of microcracks or interfacial debonding that facilitates a rapid evaporation of the absorbed water and, as a consequence, accelerates the reversible processes. As already stated, the diffusion coefficient of W30Dx batch is slightly higher than that of W15Dx, suggesting that, due to the longer exposition time to salt-fog, the

specimen has suffered slightly greater physical damages (e.g., internal cracks) which acted as preferential paths for water diffusion.

Nevertheless, the desorption trend of the batches is quite similar, indicating that both are characterized by compatible and kinetically fast desorption processes. This experimental evidence indicates that most of the phenomena favoring the water absorption during the wet phase are reversible and characterized by higher desorption kinetics than absorption one. However, this does not mean that the reversibility of the absorption/desorption phenomenon also corresponds to the reversibility of the degradation phenomena resulting from the exposition to hostile environmental conditions such as marine one. Further mechanisms not contemplated in this analysis must be taken into account, for which the discussion of the mechanical characterization can provide further information.

Furthermore, the evaluation of the composites density and their relative void content for each evaluated condition can be a suitable approach to evaluate better the material degradation induced by water uptake during salt-fog exposition.

By analyzing the evolution of the apparent density of the composite laminates (see Figure 3), it can be noticed that an increase in experimental density occurs at increasing the exposition time to salt-fog, due to the progressive water adsorption. In particular, the W15D0 specimen (exposed to salt-fog condition for 15 days) showed an increase in density of about 1.7%, in comparison to the unaged specimen (W0D0). However, the increase in composite density becomes approximately 2% higher than that of the unaged one, after 30 days in the climatic chamber (i.e. W30D0 specimen). This indicates that further water adsorption phenomena in the hydrophilic or porous regions of the composite have taken place. Moreover, kinetically secondary adsorption phenomena may have caused a further increase in the density of the laminate. It is interesting to note that, similarly to the apparent density, the void content in the laminate has a progressive increase during the wet phase. The unaged W0D0 composite exhibited a void content equal to 10.6%. This value increases up to 11.6% and 12.2% after 15 and 30 days of salt-fog exposition, respectively (i.e., W15D0 and W30D0). Furthermore, the void content significantly increases after the dry phase. The maximum void content,

equal to 13.6%, was estimated for W30D21 batch (i.e., exposed to salt-fog for 30 days and then dried for 21 days). This means that the evaporation of the absorbed water leaves cavities in the composite bulk thus causing the increase of void content and the reduction of apparent density of composites. This behavior can be justified by considering the activation of irreversible degradative phenomena on the composite constituents and/or their interface.

### 3.2 Wettability measurements

In order to evaluate how the interaction between the laminate surface with the water molecules evolves during the wet and dry aging phases, water contact angle (WCA) measurements were carried out during the different steps of the aging process. In particular, Figure 4 shows the WCA values for unaged sample as well as for W15 and W30 batches both in wet and dry conditions (W15D0-W30D0 and W15D21-W30D21, respectively). The red dotted line indicates a WCA equal to  $90^\circ$ , identified as the threshold value between hydrophilic and hydrophobic behaviors of the surface. In particular, by comparing the WCA values for all the investigated batches, it is possible to observe that:

- W0D0: The unaged composite laminate exhibits a hydrophobic behavior, evidenced by an average WCA values of about  $104.6^\circ$ . By taking into account the hydrophilic nature of the flax fiber, this result indicates that the surface properties of the composite are influenced significantly by the hydrophobic nature of the epoxy matrix. Indeed, the thermosetting resin embed the lignocellulosic reinforcement thus preventing its direct interaction with the water molecules. Therefore, the water absorption phenomenon is superficially hindered;
- W15D0: Due to the exposition to salt-fog environment for 15 days, a slight reduction in the water contact angle was observed (i.e., from  $104.6^\circ$  to  $91.9^\circ$ ). Two competing mechanisms occurred: i) the salt-fog aging test implies a further post-cure of the laminate due to the applied thermal conditions (i.e.  $35^\circ\text{C}$ ) [31]. The increase of the resin conversion due to post-curing, reduces the water diffusion, thus leading to an increase of water contact (i.e., hydrophobicity). At the same time, a gradual swelling of the fiber and subsequent damaging of the resin induces

the formation of local defects and cracks on the laminate surface [8]. Therefore, preferential pathways for the water passage are generated, thus exalting the water uptake of the samples. This contributes to improve the hydrophilic behavior of the natural fiber composite as well as to increase the water absorption capability of the composite surface (i.e., hydrophilicity) [32]. The shielding effect supplied by the resin to the water permeation is progressively compromised. The matrix has a not dominant role on the amount of water absorbed in comparison to the natural reinforcement. In fact, the high hydrophilic nature of flax fibers plays a key role in the absorption of water in the composite laminate. The higher the fiber content, the higher the amount of water absorbed [33]. Despite the occurrence of these two competing mechanisms, the observed contact angle values evidence a clear hydrophilic behavior of the composite surface, thus indicating that the damaging phenomenon has a predominant role in comparison to the post-curing one. In this regard, an important role can also be attributed to sodium chloride in the salt-fog environment. The saline solution that will be absorbed on the surface involves the deposition in the cavities of the composite surface of NaCl salt grains, which have a marked hydrophilic behavior. Consequently, a self-feeding mechanism for the absorption and diffusion of water is triggered, which further increases the water sensitivity of the composite;

- W30D0: The exposition for longer time in the salt-fog chamber leads to the triggering and growth of a relevant amount of cracks and defects [33,34], which involves a great modification of the surface wettability. Hence, the WCA average value found for these specimens is approximately  $11^\circ$  lower than that of the W15D0 ones (i.e.,  $80.8^\circ$  versus  $91.9^\circ$ , respectively);
- W15D21/W30D21: The drying cycle favors a recovery of the hydrophobic properties, already highlighted by unaged specimens. However, both softening and degradation phenomena experienced during the wet phase by both constituents (i.e., epoxy resin and flax fiber) and their interface, have led to an irreversible modification of the composite wettability. As a

consequence, both laminates show slightly higher affinity with water in comparison to W0D0 one (i.e., unaged). Indeed, after 21 days of drying the contact angles average values becomes respectively equal to  $99.4^\circ$  and  $90.9^\circ$  for W15 and W30 batches, with reductions of  $5.2^\circ$  and  $13.7^\circ$  in comparison to the unaged sample. This behavior could be attributed to the presence of cracks, voids and surface defects, which remain on the surface even after the water evaporation occurred during the dry phase. This results in a direct exposure of flax fibers, which increases surface hydrophilicity.

It is worth noting that samples aged under salt-fog for 30 days (i.e., W30D0 and W30D21) showed the higher error bar, indicating a larger dispersion of data. This behavior can be related to the higher surface damaging induced by a longer duration of the wet phase. As already stated, the exposition to salt-fog can trigger surface defects and voids that locally expose flax fibers, thus increasing the hydrophilicity of the composite laminate. The high heterogeneity on surface energy in the sample has consequently caused a large standard deviation of WCA values in W30D0 and W30D21 batches.

### **3.3 Scheme of the hydration/dehydration induced degradation mechanisms**

Several phenomena contribute simultaneously to stimulate the formation of defects or cavities which imply an increment in the void content of the composite laminate. A simplified scheme of the degradation mechanisms is shown in Figure 5. The water molecules permeate inside the composite structure by diffusion mechanism. The hydrophilic areas (Figure 5a, point a1) of the thermosetting matrix can be considered as local preferential pathways for the water diffusion (Figure 5b, point b1) [25]. Moreover, some authors ascribed the quite high moisture adsorption of the bisphenol A diglycidyl ether epoxy resin (i.e., DGEBA) to their high crosslink density and, as a consequence, to the limited chain mobility, which make these systems less compact (i.e., having high free volume) [35–37]. This favors the triggering of voids or cavities within the matrix. Furthermore, micro-defects (in Figure 5a, point a2) or cracks (Figure 5a, point a3) intrinsically generated in the matrix during the manufacturing process or due to capillarity water diffusion at the fiber/matrix interface exalt the

diffusion rate (in Figure 5b, point b2). Similarly, debonding and delamination phenomena can take place at the fiber-matrix interface [5]. Natural fiber swelling (in Figure 5c, point c1) leads to an increase of internal stresses at the fiber-matrix interface that is partially reduced by matrix cracks or molecules relaxation (in Figure 5c, point c2) [38]. These stresses favor interfacial debonding and delamination already during the absorption stage leading to a further increase of the water uptake. Furthermore, flax fiber reinforced composites experienced a noticeable desorption of water (i.e., in the range 6-8%) during the dry phase (see Figure 1). This implies a relevant shrinkage of flax fibers, which leads to local detachments of the polymer matrix from the fiber (in Figure 5d, point d1). In addition, local dissolution of soluble constituents (e.g. hydrocarbons, waxes and lignin) of flax in water solution improved the amount of defects on the surface of the natural fiber [15]. The shrinkage process in the fiber is more relevant than in the matrix [39], thus enhancing the composite damaging induced by water. The generated interfacial stress, due to this mismatch between fiber and matrix shrinkage, is released by the nucleation and growth of other micro cracks in both matrix and fibers as well as at the fiber-matrix interface (Figure 5d, point d2) [6]. The so created large debonded area noticeably worsens the interfacial mechanical properties of laminates in addition to exalt the water vapor mass diffusion during its evaporation in the dry phase. This finding is in complete agreement with the experimental result concerning the higher desorption rate than adsorption one.

### 3.4 Quasi-static mechanical tests

With the aim of defining a reference to assess the mechanical performances recovery of flax composites during the dry phase, the evolution of flexural stress-strain curves at varying the exposition time to salt-fog (i.e., wet phase) was preliminarily shown in Figure 6. As reported in the literature [40], the water absorption involves a progressive softening of natural fiber reinforced composites, which implies a reduction in the maximum strength and stiffness as well as an increase in the deformation at break. This behavior can be attributed to a synergistic and concomitant action of various degradative phenomena, which contribute to the worsening of the composite performances.

As clearly evidenced in Figure 6, the absorbed moisture has an extensive effect on the mechanical response of flax fiber reinforced composites leading to relevant modifications in the stress-strain curve. It is worth noting that, by evaluating Figure 6, W15D0 and W30D0 composites showed substantial reductions in both flexural strength (i.e., equal of -28.7% and -31.5%) and flexural modulus (i.e., equal to -60.1% and 63.6%) in comparison to the unaged ones (i.e. W0D0), respectively. At the same time, a noticeable increase of the strain at break was also observed. The strength and stiffness reductions can be mainly related to the degradation phenomena triggered by the noticeable water sorption (see Figure 1) experienced by flax fiber reinforced composites during the salt-fog exposition. Indeed, the absorption of large amount of water causes matrix micro-cracking due to the swelling of flax fibers [23], which implies a decrease in the threshold strength for the crack activation and propagation in the composite [40]. Similarly, the relevant increase in the strain at break can be associated with a softening and plasticization effect of the wet composite sample [29]. It is also important to underline that, by observing the stress-strain curves, a transition from predominantly linear mode with catastrophic fracture to non-linear mode with progressive fracture can be identified at increasing the salt-fog exposition time. This suggests, considering the high deformation values reached by the investigated composites during the bending tests, the occurrence of high interlaminar damages which generate shear and delamination fractures between the laminae, thus leading to a ductile failure mode [41]. However, there are controversial opinions in the literature about the role of fiber-matrix adhesion worsening in the reduction of composites performances. Nevertheless, there is a common address that the interfacial fiber-matrix resistance surely influences the mechanical behavior of the laminate at different times of aging [42].

These considerations are confirmed by analyzing the flexural fracture methods of the specimens as the immersion time in the salt spray chamber increases (Figure 7). The unaged sample (W0D0) shows a sharp and sudden fracture which starts in the external laminae that suffer the maximum tensile stress. Then, it rapidly propagates longitudinally towards the center of the specimen. In the sample exposed to salt-fog for 15 days (i.e., W15D0), secondary fracture mechanisms, attributable to the



increased ductility of the material and the reduction of interlaminar strength, are identifiable by observing the fracture surface. Hence, a partial propagation of the fracture crack transversely to the applied load direction occurs, ascribed to delamination and interlaminar shear fractures. On the other hand, for the specimen subjected to a 30-day wet phase, the composite plasticization, induced by the significant water absorption, did not allow to detect a clear fracture surface also at great deflection values (as confirmed by evaluating the stress-strain curve in Figure 6).

It is worth underlining that not all the aging mechanisms induce an irreversible damage in the composite laminate. As clearly shown in Figure 1, the dry phase carried out under controlled conditions (i.e., 50% U.R. and 22°C) involves a progressive desorption of the water previously absorbed by the samples during the salt-fog exposition (i.e., wet phase of the aging cycle). After the wet phase, a progressive recovery of the mechanical performances is expected by considering that the degradation mechanisms may be reversible or irreversible. The discrimination and quantification of the performance reversibility during the dry phase is a relevant information for a reliable durability design of this class of composite laminates.

Figure 8 shows the stress-strain curves at increasing drying time of samples exposed to salt-fog for (a) 15 days and (b) 30 days. As already stated, after 15 days under salt-fog environmental conditions W15D0 composites showed clear decreases in terms of both flexural strength and stiffness as well as a noticeable increment in the deformation at break. Figure 9 highlights that W30D0 sample did not show an evident flexural fracture in the span centerline. However, the specimen suffered a relevant deflection without leading to the triggering of critical failure cracks in the fiber and matrix thanks to the significant elastoplastic behavior offered by the wet aged constituents. The following dry phase allows to progressively recover its mechanical performances (Figure 8a): i.e., a partial enhancement of the maximum flexural strength in addition to a decrease of the strain at failure. Furthermore, it is important to underline that the initial slope of the curve (i.e., evaluated at low strain values) related to the flexural modulus of the laminate, undergoes a progressive increase. This means that degradative phenomena such plasticization and softening due to the wet phase can be considered as partially

reversible. In particular, the laminate experienced after the dry phase an almost complete recovery of the maximum flexural strength: i.e., W15D21 sample shows an average value of the maximum strength equal to 72.6 MPa, i.e., 2.6% lower than unaged one (i.e., W0D0). Furthermore, the strain at failure of the W15D21 sample is equal to 10.5%, significantly higher (+73%) than that shown by W0D0 sample. As shown in Figure 8b, similar considerations can be drawn by observing the effect of the dry phase on the mechanical behavior of the specimens exposed to salt-fog for 30 days (i.e., W30Dx).

Lateral and bottom views of the flexural fracture surface of W30D1 and W30D21 samples (Figure 9) confirms these findings. The failure starts for tensile fracture of the external bottom laminae (see bottom views in Figure 9). Afterward, it progressively propagates toward the centre of the sample, causing somewhere debonding and pull-out of the upper texture fabrics as well as interlaminar shear fracture (identifiable by the horizontally oriented red arrows – lateral view images in Figure 9).

This suggests that the degradation phenomena triggered by the water absorption during the wet phase have a coupled reversible and irreversible contribution that can affect the mechanical properties of the resulting composites in different ways. Quite interestingly, the laminate still preserves a high ductility at the end of the dry phase, indicating that its stiffness is just partially compromised. Conversely, the stress limit can be considered largely recovered. Consequently, the strength reduction experienced during the wet phase can be ascribed to mainly reversible aging phenomena whereas the stiffness loss is more probably correlated to both reversible and irreversible degradative phenomena. The water absorbed in the epoxy resin is identifiable as free or bound water [43]. The former is referred to the water molecules able to flow and diffuse through the voids and/or pores in the matrix. Vice versa, the latter concerns the water molecules bonded to polar groups of the polymeric network [44].

Furthermore, due to the hydrophilic behavior of natural fibers, flax fibers swell significantly higher than the surrounding epoxy matrix. Hence, a radial stress could be generated at the fiber-matrix interface, thus creating interfacial micro-cracks in the matrix as well as leading to local fiber/matrix

debonding [28]. All these factors can contribute to the strength reduction of the composite laminate experienced during the wet phase of the aging cycle.

Vice versa, the reduction in the composite stiffness could be ascribed to a synergistic action of softening phenomena involving both matrix and fibers. Indeed, dry flax fiber consists of quite rigid cellulose fibrils with the cellulose molecules stably bonded within these fibrils. However, water can diffuse by capillarity through cellulose network and penetrate in the fibrils. Hence, the water molecules can interact with the flax fiber in correspondence of the hydroxyl terminated groups of the cellulose molecules, thus forming hydrogen bonds [45]. As a consequence, this interaction leads to the reduction of the bonding forces that make the flax structure rigid. The water therefore acts as a plasticizer allowing the cellulose molecules to move and increasing the flexibility of the fiber [46].

Figure 10 confirms the capability of the flax fiber reinforced composite to noticeably recover its mechanical properties reduction experienced during the wet phase (i.e., salt-fog exposition), thanks to the following dry phase. As already discussed, this means that both reversible and irreversible aging phenomena play an important role in the worsening of the mechanical response during the wet phase. Quite interestingly, the laminate showed an almost complete recovery of the flexural strength at the end of the dry phase. In particular, Figure 10a shows that composites exposed to salt-fog for 15 days (i.e., W15Dx) and 30 days (i.e., W30Dx) were able, at the end of the dry phase (i.e., 21 days), to recover more than 99% and 97.5% of their initial flexural strength values, respectively. On the other hand, the 78% and the 69.4% of the flexural modulus was recovered by the same composites after 21 days of drying.

These findings clearly evidence that the flexural load carrying capacity of flax fiber reinforced composites is more strictly related to mainly reversible degradative phenomena whereas the stiffness loss is more probably correlated to irreversible ones.

In order to deeper understand the evolution of the mechanical response of the composites after wet (i.e., salt fog exposition) and dry phases, SEM images of some flexural fractured specimen were collected, and the micrographs taken at a magnification level of 200x are reported in Figure 11.

From a morphological point of view, the W0D0 sample is characterized by flax fibers properly embedded in the epoxy resin. The matrix penetrates in the interstices among fibers allowing a continuous connection with the reinforcement. This leads to a proper stress distribution at the fiber/matrix interface, thus also avoiding the presence of interfacial cavities or macroscopic defects in the matrix. Nevertheless, W30D0 laminate exhibits a quite irregular morphology. The flax fiber bundle is unraveled with evidence of local defects or interfacial debonding. The absorbed water weakens the physical and chemical interfacial bonds, thus provoking debonding phenomena [32]. This implies that preferential pathways for water diffusion were constituted at the fiber/matrix interface, thus favoring a premature degradation of the flax fiber reinforced composite laminate. These heterogeneities represent a relevant structural discontinuity which are also present at the end of the dry phase. Hence, the reduced fiber-matrix interfacial adhesion causes an ineffective stress transfer among the constituents thus strongly influencing the stiffness as well as increasing the ductility and toughness of the composite laminate [47,48]. Moreover, the presence of defects or cracks in the polymeric matrix favors a reduction in the critical stress at failure of the composite.

In order to get further insights concerning the performance variation of the laminate, a topological map (i.e., reversibility map), able to discriminate reversible and irreversible aging zones, was created. Figure 12 represents the reversibility map referred to the flexural modulus experimental data (see for reference Figure 10b). The solid blue line is related to the aging curve of the composite at increasing the exposition time in the salt-fog environment. The region below this line represents a state of over-aging which resulted in a decrease in performance greater than the experimentally estimated one. On the other hand, the solid black line discriminates the reversible and irreversible aging zones. This curve can be obtained by joining the points at equilibrium at the end of each dry phase with the unaged one. It is important to underline that for flax fiber reinforced composites most of the aging phenomena are reversible (see the area with green arrows shown in Figure 12). The region highlighted in red represents the area related to the irreversible aging. This region becomes the more relevant the longer the exposition time to the salt-fog chamber.

This graph can be used in the design to estimate the performance decay and the recovery conditions due to a wet-dry aging cycle. For example, by considering the time duration of the wet phase equal to 23 days, a reduction in the laminate performance of about 65% can be expected (point 1 in the Figure 12). However, by following reversibility curves during the dry phase (i.e., dotted red arrow in Figure 12), a partial performance recovery can be predicted with a final residual decay at long drying times lower than 30% (i.e., point 2 in Figure 12). This indicates that a recovery of this properties equal to about 35% can be expected at the end of the dry phase.

These findings mean that degradation phenomena which take place during the humid aging phase do not necessarily imply a permanent deterioration in the laminate performance. A relationship between reversible and irreversible degradation processes on the durability issues of the investigated composite laminates can be identified. In particular, the irreversible contribution is all the more relevant the longer the aging time is imposed. Future studies, aimed to better discriminate the phenomena related to the triggering and propagation of irreversible degradation mechanisms, will further enhance the achieved results.

## Conclusion

The main goal of the present paper is to investigate the ability of flax fiber reinforced composites in the recovery of their mechanical performances under partially similar marine environment. To this aim, composites manufactured through vacuum infusion were aged under salt-fog at 35 °C for 15 and 30 days, respectively. After the initial wet phase, the aged materials were stored in “dry” condition (i.e., 50% R.H. and 22°C) for an interval time varying between 1 and 21 days. The performances evolution was evaluated by performing quasi-static mechanical tests, water uptake and water contact angle measurements on both unaged and aged samples. Moreover, the surface morphology of fractured surfaces after flexural testing was examined by using 3D optical microscope and scanning electron microscope (SEM).

It was found that flax fiber reinforced composites experience phenomena of both reversible and irreversible degradation during the wet phase thus evidencing a relevant mechanical recovery at the end of the dry phase. In particular, the mechanical characterization revealed that the laminates exposed to salt-fog for 30 days are able to recover more than 99% and about the 78% of their initial flexural strength and modulus values after 21 days of drying, respectively.

These results were summarized in a topological reversibility map of the mechanical behavior able to visually quantify both reversible and irreversible degradative contribute in the NFRC performances. These findings clearly evidenced that the flexural load carrying capacity of the investigated composites is more closely related to mainly reversible aging phenomena whereas the stiffness loss to irreversible ones.

## **Acknowledgements**

This research follows from Project “SI-MARE – Soluzioni Innovative per Mezzi navali ad Alto Risparmio Energetico” (P.O. FESR Sicilia 2014/2020).

Journal Pre-proof

## Reference

- [1] Yan L, Chouw N, Jayaraman K. Flax fibre and its composites – A review. *Compos Part B Eng* 2014;56:296–317. <https://doi.org/10.1016/j.compositesb.2013.08.014>.
- [2] Le Duigou A, Bourmaud A, Davies P, Baley C. Long term immersion in natural seawater of Flax/PLA biocomposite. *Ocean Eng* 2014;90:140–8. <https://doi.org/10.1016/j.oceaneng.2014.07.021>.
- [3] Yan L, Chouw N. Effect of water, seawater and alkaline solution ageing on mechanical properties of flax fabric/epoxy composites used for civil engineering applications. *Constr Build Mater* 2015;99:118–27. <https://doi.org/10.1016/j.conbuildmat.2015.09.025>.
- [4] Le Duigou A, Davies P, Baley C. Seawater ageing of flax/poly(lactic acid) biocomposites. *Polym Degrad Stab* 2009;94:1151–62. <https://doi.org/10.1016/j.polymdegradstab.2009.03.025>.
- [5] Dhakal HN, Zhang ZY, Richardson MOW. Effect of water absorption on the mechanical properties of hemp fibre reinforced unsaturated polyester composites. *Compos Sci Technol* 2007;67:1674–83. <https://doi.org/10.1016/j.compscitech.2006.06.019>.
- [6] Moudood A, Rahman A, Öchsner A, Islam M, Francucci G. Flax fiber and its composites: An overview of water and moisture absorption impact on their performance. *J Reinf Plast Compos* 2019;38:323–39. <https://doi.org/10.1177/0731684418818893>.
- [7] Oksman K, Skrifvars M, Selin J-F. Natural fibres as reinforcement in polylactic acid (PLA) composites. *Compos Sci Technol* 2003;63:1317–24. [https://doi.org/10.1016/S0266-3538\(03\)00103-9](https://doi.org/10.1016/S0266-3538(03)00103-9).
- [8] Fiore V, Calabrese L, Di Bella G, Scalici T, Galtieri G, Valenza A, et al. Effects of aging in salt spray conditions on flax and flax/basalt reinforced composites: Wettability and dynamic mechanical properties. *Compos Part B Eng* 2016;93:35–42.



- <https://doi.org/10.1016/j.compositesb.2016.02.057>.
- [9] Fiore V, Scalici T, Badagliacco D, Enea D, Alaimo G, Valenza A. Aging resistance of bio-epoxy jute-basalt hybrid composites as novel multilayer structures for cladding. *Compos Struct* 2017;160:1319–28. <https://doi.org/10.1016/j.compstruct.2016.11.025>.
- [10] Fiore V, Scalici T, Sarasini F, Tirilli J, Calabrese L. Salt-fog spray aging of jute-basalt reinforced hybrid structures: Flexural and low velocity impact response. *Compos Part B Eng* 2017;116:99–112. <https://doi.org/10.1016/j.compositesb.2017.01.031>.
- [11] Saidane EH, Scida D, Assarar M, Sabhi H, Ayad R. Hybridisation effect on diffusion kinetic and tensile mechanical behaviour of epoxy based flax–glass composites. *Compos Part A Appl Sci Manuf* 2016;87:153–60. <https://doi.org/10.1016/j.compositesa.2016.04.023>.
- [12] Calabrese L, Fiore V, Bruzzaniti P, Scalici T, Valenza A. Pinned hybrid glass-flax composite laminates aged in salt-fog environment: Mechanical durability. *Polymers (Basel)* 2020;12. <https://doi.org/10.3390/polym12010040>.
- [13] Fiore V, Sanfilippo C, Calabrese L. Dynamic Mechanical Behavior Analysis of Flax/Jute Fiber-Reinforced Composites under Salt-Fog Spray Environment. *Polymers (Basel)* 2020;12:716. <https://doi.org/10.3390/polym12030716>.
- [14] Thwe MM, Liao K. Effects of environmental aging on the mechanical properties of bamboo–glass fiber reinforced polymer matrix hybrid composites. *Compos Part A Appl Sci Manuf* 2002;33:43–52. [https://doi.org/10.1016/S1359-835X\(01\)00071-9](https://doi.org/10.1016/S1359-835X(01)00071-9).
- [15] Fiore V, Scalici T, Calabrese L, Valenza A, Proverbio E. Effect of external basalt layers on durability behaviour of flax reinforced composites. *Compos Part B Eng* 2016;84:258–65. <https://doi.org/10.1016/j.compositesb.2015.08.087>.
- [16] Jain D, Kamboj I, Bera TK, Kang AS, Singla RK. Experimental and numerical investigations on the effect of alkaline hornification on the hydrothermal ageing of Agave natural fiber composites. *Int J Heat Mass Transf* 2019;130:431–9. <https://doi.org/10.1016/j.ijheatmasstransfer.2018.10.106>.

- [17] Wang X, Petru M, Yu H. The effect of surface treatment on the creep behavior of flax fiber reinforced composites under hygrothermal aging conditions. *Constr Build Mater* 2019;208:220–7. <https://doi.org/10.1016/j.conbuildmat.2019.03.001>.
- [18] Chen D, Li J, Ren J. Influence of fiber surface-treatment on interfacial property of poly(l-lactic acid)/ramie fabric biocomposites under UV-irradiation hydrothermal aging. *Mater Chem Phys* 2011;126:524–31. <https://doi.org/10.1016/j.matchemphys.2011.01.035>.
- [19] El-Abbassi FE, Assarar M, Ayad R, Lamdouar N. Effect of alkali treatment on Alfa fibre as reinforcement for polypropylene based eco-composites: Mechanical behaviour and water ageing. *Compos Struct* 2015;133:451–7. <https://doi.org/10.1016/j.compstruct.2015.07.112>.
- [20] Fiore V, Sanfilippo C, Calabrese L. Influence of sodium bicarbonate treatment on the aging resistance of natural fiber reinforced polymer composites under marine environment. *Polym Test* 2019;80:106100. <https://doi.org/10.1016/j.polymertesting.2019.106100>.
- [21] Swain PTR, Biswas S. A comparative analysis of physico-mechanical, water absorption, and morphological behaviour of surface modified woven jute fiber composites. *Polym Compos* 2018;39:2952–60. <https://doi.org/10.1002/pc.24294>.
- [22] Ventura H, Claramunt J, Navarro A, Rodriguez-Perez MA, Ardanuy M. Effects of wet/dry-cycling and plasma treatments on the properties of flax nonwovens intended for composite reinforcing. *Materials (Basel)* 2016;9:1–18. <https://doi.org/10.3390/ma9020093>.
- [23] Cadu T, Van Schoors L, Sicot O, Moscardelli S, Divet L, Fontaine S. Cyclic hygrothermal ageing of flax fibers' bundles and unidirectional flax/epoxy composite. Are bio-based reinforced composites so sensitive? *Ind Crops Prod* 2019;141:111730. <https://doi.org/10.1016/j.indcrop.2019.111730>.
- [24] Van Schoors L, Cadu T, Moscardelli S, Divet L, Fontaine S, Sicot O. Why cyclic hygrothermal ageing modifies the transverse mechanical properties of a unidirectional epoxy-flax fibres composite? *Ind Crops Prod* 2021;164:113341. <https://doi.org/10.1016/j.indcrop.2021.113341>.
- [25] Zhou J, Lucas JP. Hygrothermal effects of epoxy resin. Part I: the nature of water in epoxy.

- Polymer (Guildf) 1999;40:5505–12. [https://doi.org/10.1016/S0032-3861\(98\)00790-3](https://doi.org/10.1016/S0032-3861(98)00790-3).
- [26] Karad SK, Attwood D, Jones FR. Moisture absorption by cyanate ester modified epoxy resin matrices. Part V: Effect of resin structure. *Compos Part A Appl Sci Manuf* 2005;36:764–71. <https://doi.org/10.1016/j.compositesa.2004.10.022>.
- [27] Assarar M, Scida D, El Mahi A, Poilâne C, Ayad R. Influence of water ageing on mechanical properties and damage events of two reinforced composite materials: Flax-fibres and glass-fibres. *Mater Des* 2011;32:788–95. <https://doi.org/10.1016/j.matdes.2010.07.024>.
- [28] Moudood A, Rahman A, Khanlou HM, Hall W, Öchsner A, Francucci G. Environmental effects on the durability and the mechanical performance of flax fiber/bio-epoxy composites. *Compos Part B Eng* 2019;171:284–93. <https://doi.org/10.1016/j.compositesb.2019.05.032>.
- [29] Stamboulis A, Baillie CA, Peijs T. Effects of environmental conditions on mechanical and physical properties of flax fibers. *Compos Part A Appl Sci Manuf* 2001;32:1105–15. [https://doi.org/10.1016/S1359-835X\(01\)00032-X](https://doi.org/10.1016/S1359-835X(01)00032-X).
- [30] Mercier J, Bunsell A, Castaing P, Renard J. Characterisation and modelling of aging of composites. *Compos Part A Appl Sci Manuf* 2008;39:428–38. <https://doi.org/10.1016/j.compositesa.2007.08.015>.
- [31] Mourad AHI, Beckry Mohamed AM, El-Maaddawy T. Effect of seawater and warm environment on glass/epoxy and glass/polyurethane composites. *Appl Compos Mater* 2010;17:557–73. <https://doi.org/10.1007/s10443-010-9143-1>.
- [32] Calabrese L, Fiore V, Scalici T, Valenza A. Experimental assessment of the improved properties during aging of flax/glass hybrid composite laminates for marine applications. *J Appl Polym Sci* 2019;136:47203. <https://doi.org/10.1002/app.47203>.
- [33] Espert A, Vilaplana F, Karlsson S. Comparison of water absorption in natural cellulosic fibres from wood and one-year crops in polypropylene composites and its influence on their mechanical properties. *Compos Part A Appl Sci Manuf* 2004;35:1267–76. <https://doi.org/10.1016/j.compositesa.2004.04.004>.

- [34] Pandian A, Vairavan M, Jebbas Thangaiah WJ, Uthayakumar M. Effect of Moisture Absorption Behavior on Mechanical Properties of Basalt Fibre Reinforced Polymer Matrix Composites. *J Compos* 2014;2014:1–8. <https://doi.org/10.1155/2014/587980>.
- [35] Starkova O, Buschhorn ST, Mannov E, Schulte K, Aniskevich A. Water transport in epoxy/MWCNT composites. *Eur Polym J* 2013;49:2138–48. <https://doi.org/10.1016/j.eurpolymj.2013.05.010>.
- [36] Alessi S, Caponetti E, Güven O, Akbulut M, Spadaro G, Spinella A. Study of the curing process of DGEBA epoxy resin through structural investigation. *Macromol Chem Phys* 2015;216:538–46. <https://doi.org/10.1002/macp.201400510>.
- [37] Toscano A, Pitarresi G, Scafidi M, Di Filippo M, Spadaro G, Alessi S. Water diffusion and swelling stresses in highly crosslinked epoxy matrices. *Polym Degrad Stab* 2016;133:255–63. <https://doi.org/10.1016/j.polymdegradstab.2016.09.004>.
- [38] Newman RH. Auto-accelerative water damage in an epoxy composite reinforced with plain-weave flax fabric. *Compos Part A Appl Sci Manuf* 2009;40:1615–20. <https://doi.org/10.1016/j.compositesa.2009.07.010>.
- [39] Anand P, Rajesh D, Senthil Kumar M, Saran Raj I. Investigations on the performances of treated jute/Kenaf hybrid natural fiber reinforced epoxy composite. *J Polym Res* 2018 254 2018;25:1–9. <https://doi.org/10.1007/S10965-018-1494-6>.
- [40] Moudood A, Rahman A, Öchsner A, Islam M, Francucci G. Flax fiber and its composites: An overview of water and moisture absorption impact on their performance: *J Reinf Plast Compos* 2019;38:323–39. <https://doi.org/10.1177/0731684418818893>.
- [41] Haghghatnia T, Abbasian A, Morshedian J. Hemp fiber reinforced thermoplastic polyurethane composite: An investigation in mechanical properties. *Ind Crops Prod* 2017;108:853–63. <https://doi.org/10.1016/j.indcrop.2017.07.020>.
- [42] Muñoz E, García-Manrique JA. Water absorption behaviour and its effect on the mechanical properties of flax fibre reinforced bioepoxy composites. *Int J Polym Sci* 2015;2015.

<https://doi.org/10.1155/2015/390275>.

- [43] Azwa ZN, Yousif BF, Manalo AC, Karunasena W. A review on the degradability of polymeric composites based on natural fibres. *Mater Des* 2013;47:424–42. <https://doi.org/10.1016/j.matdes.2012.11.025>.
- [44] Maggana C, Pissis P. Water sorption and diffusion studies in an epoxy resin system. *J Polym Sci Part B Polym Phys* 1999;37:1165–82. [https://doi.org/10.1002/\(SICI\)1099-0488\(19990601\)37:11<1165::AID-POLB11>3.0.CO;2-E](https://doi.org/10.1002/(SICI)1099-0488(19990601)37:11<1165::AID-POLB11>3.0.CO;2-E).
- [45] Ray D, Rout J. Thermoset biocomposites. *Nat. Fibers, Biopolym. Biocomposites*, CRC Press; 2005, p. 291–345. <https://doi.org/10.1201/9780203508206.ch9>.
- [46] Alomayri T, Assaedi H, Shaikh FUA, Low IM. Effect of water absorption on the mechanical properties of cotton fabric-reinforced geopolymer composites. *J Asian Ceram Soc* 2014;2:223–30. <https://doi.org/10.1016/j.jascer.2014.05.005>.
- [47] Yan L. Effect of alkali treatment on vibration characteristics and mechanical properties of natural fabric reinforced composites. *J Reinf Plast Compos* 2012;31:887–96. <https://doi.org/10.1177/0731684412449399>.
- [48] Habibi M, Lebrun G, Laperrière L. Experimental characterization of short flax fiber mat composites: tensile and flexural properties and damage analysis using acoustic emission. *J Mater Sci* 2017;52:6567–80. <https://doi.org/10.1007/s10853-017-0892-1>.

## Figure captions

**Figure 1. Water uptake evolution at increasing time during wet (solid line) and dry (dotted line) phases for batch A (blue line) and batch B (red line)**

**Figure 2. Water (a) absorption and desorption of (b) W15 and (c) W30 batches**

**Figure 3. Density and void content values of unaged and aged composites**

**Figure 4. Water contact angle (WCA) of unaged and aged composites**

**Figure 5. Schematization of wet-dry degradation mechanisms (modified from [44])**

**Figure 6. Stress-strain curves for unaged (i.e., W0D0) and aged (i.e., W15D0 and W30D0) composites**

**Figure 7. Optical 3D images of flexural fractures (lateral and bottom views) for W0D0, W15D0 and W30D0 composites**

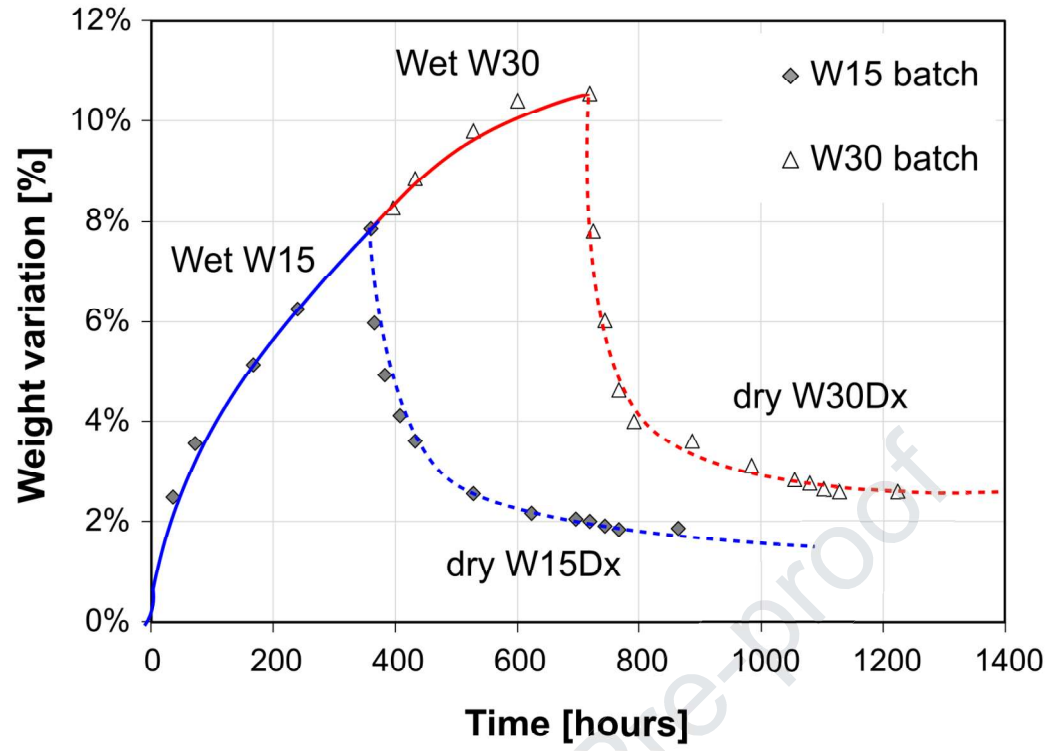
**Figure 8. Stress-strain curves at increasing drying time for samples aged for a) 15 days (i.e., W15Dx) and b) 30 days (i.e., W30Dx). As reference unaged sample was added.**

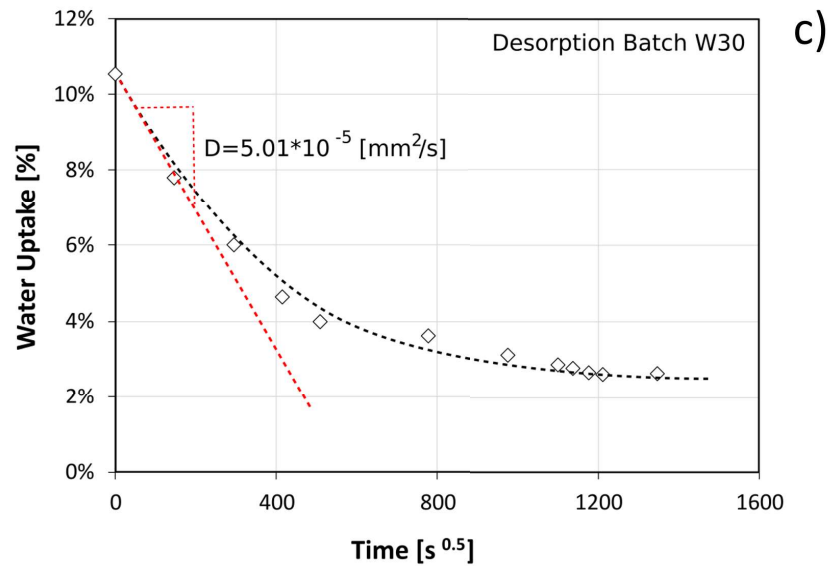
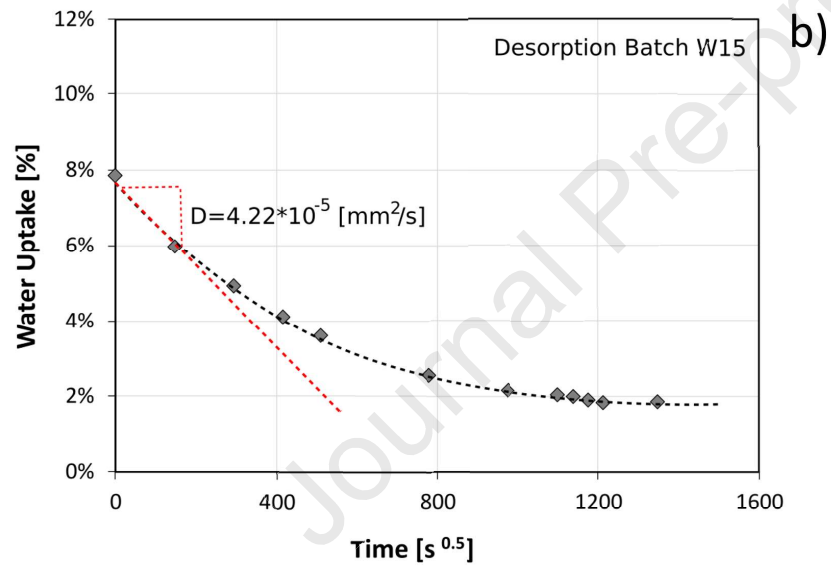
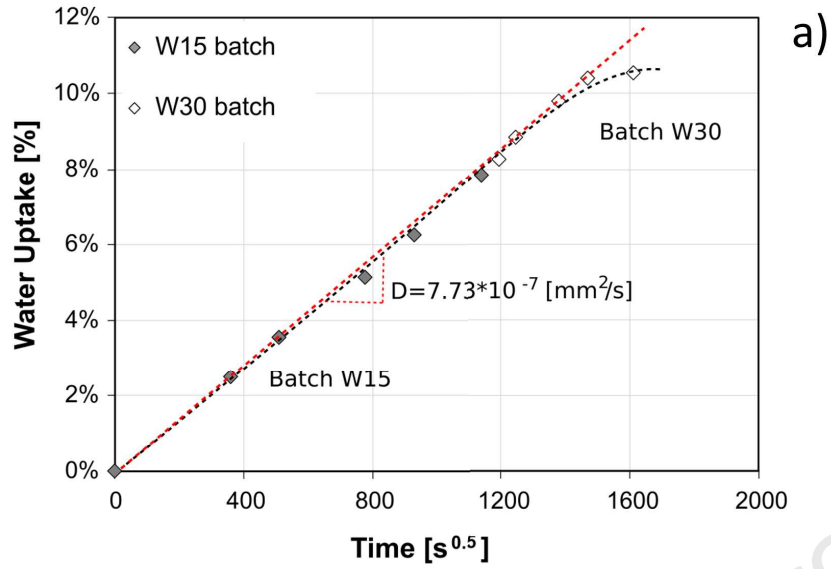
**Figure 9. Optical 3D images of flexural fractures (lateral and bottom views) for W30D0, W30D1 and W30D21 composites**

**Figure 10. Percentage variations of (a) flexural strength and (b) modulus of composites at varying time**

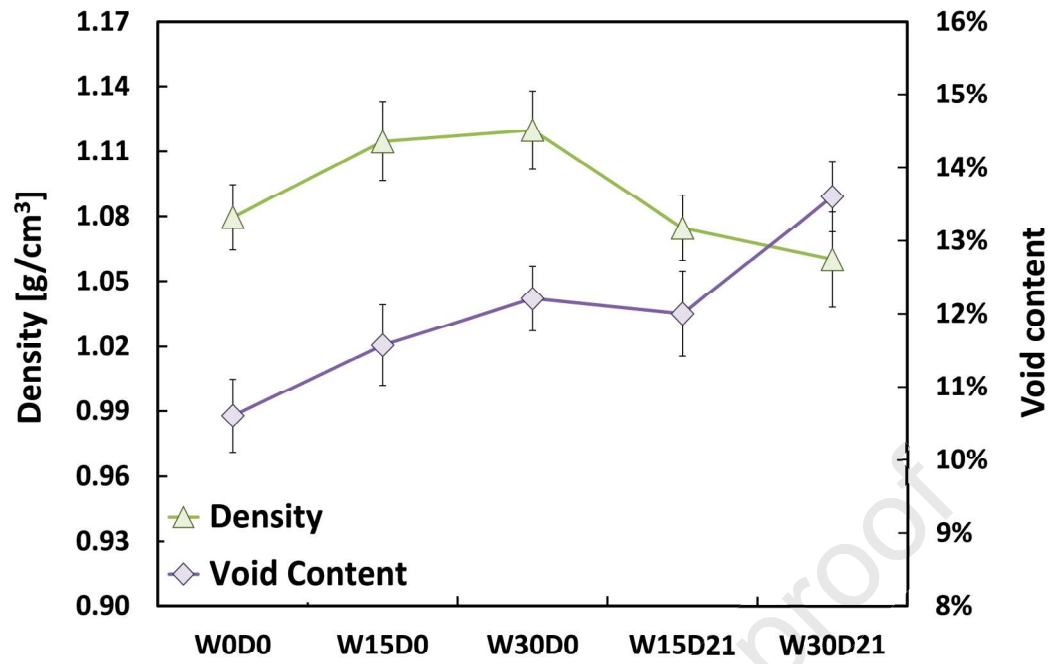
**Figure 11. SEM images of flax bundles in a) W0D0 and b) W30D21 composites**

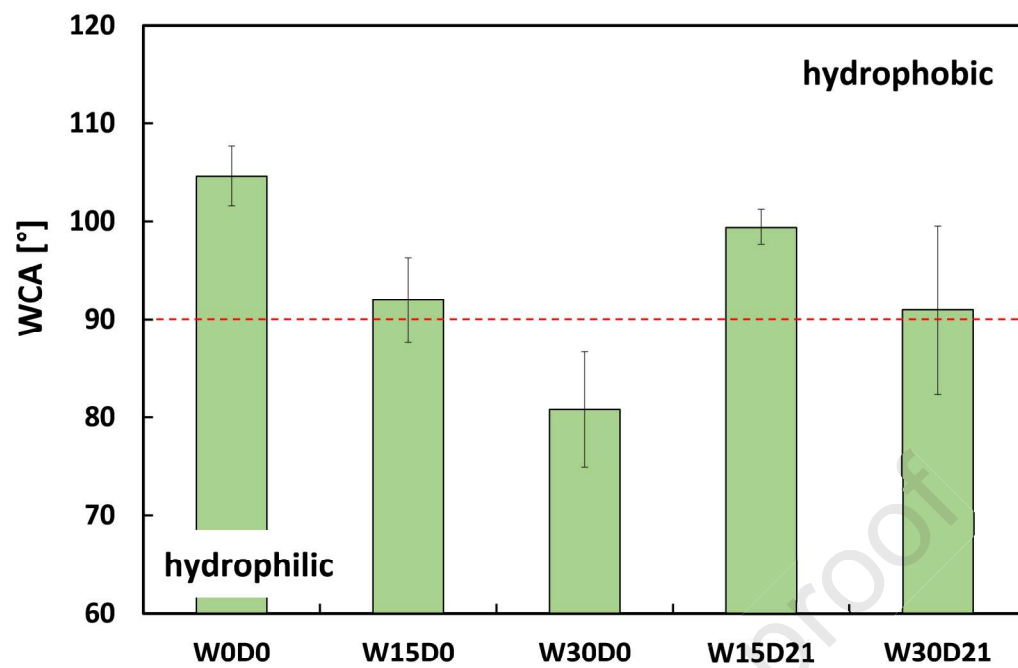
**Figure 12. Topological map for the reversibility of flexural modulus**



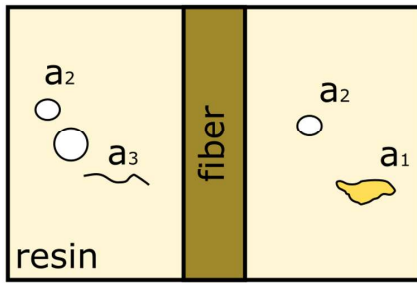




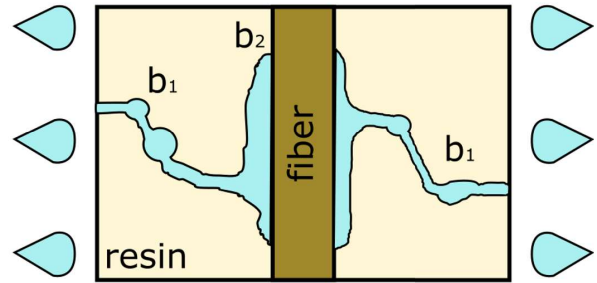




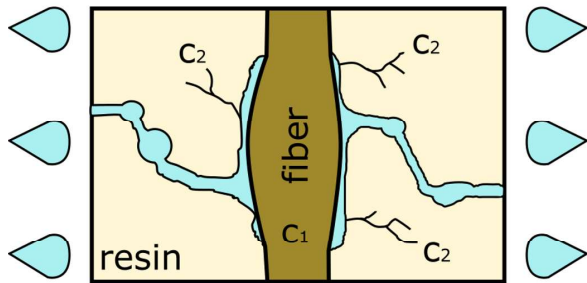
a)



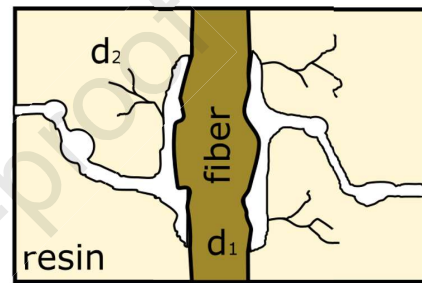
b)

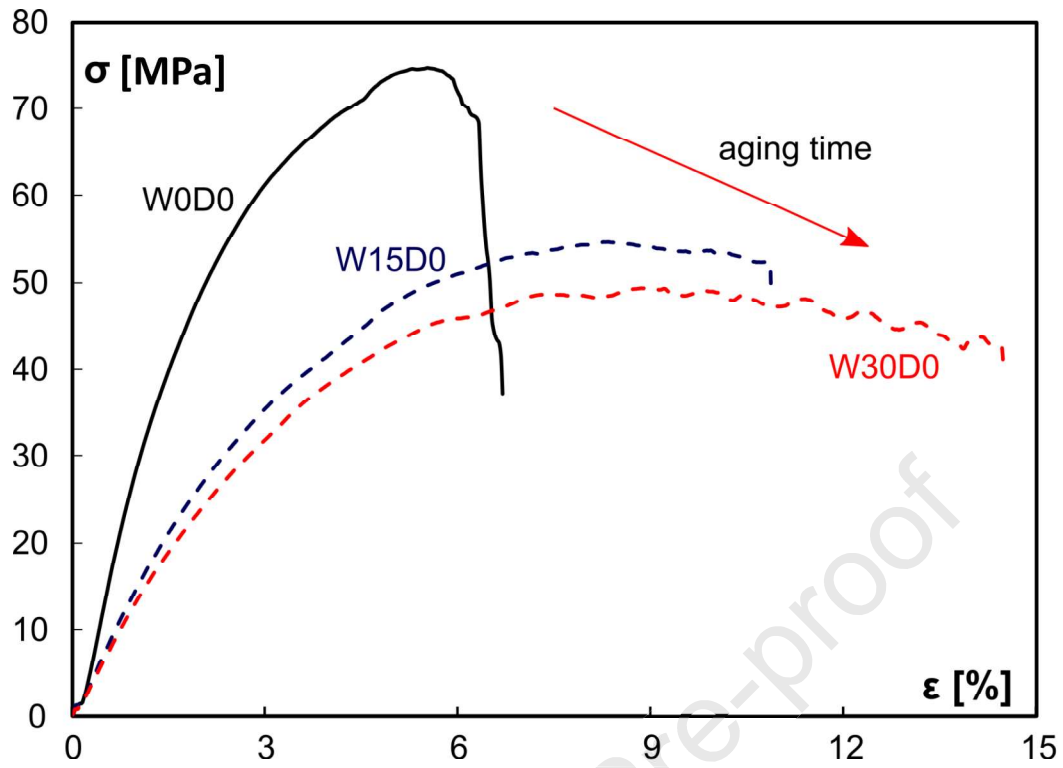


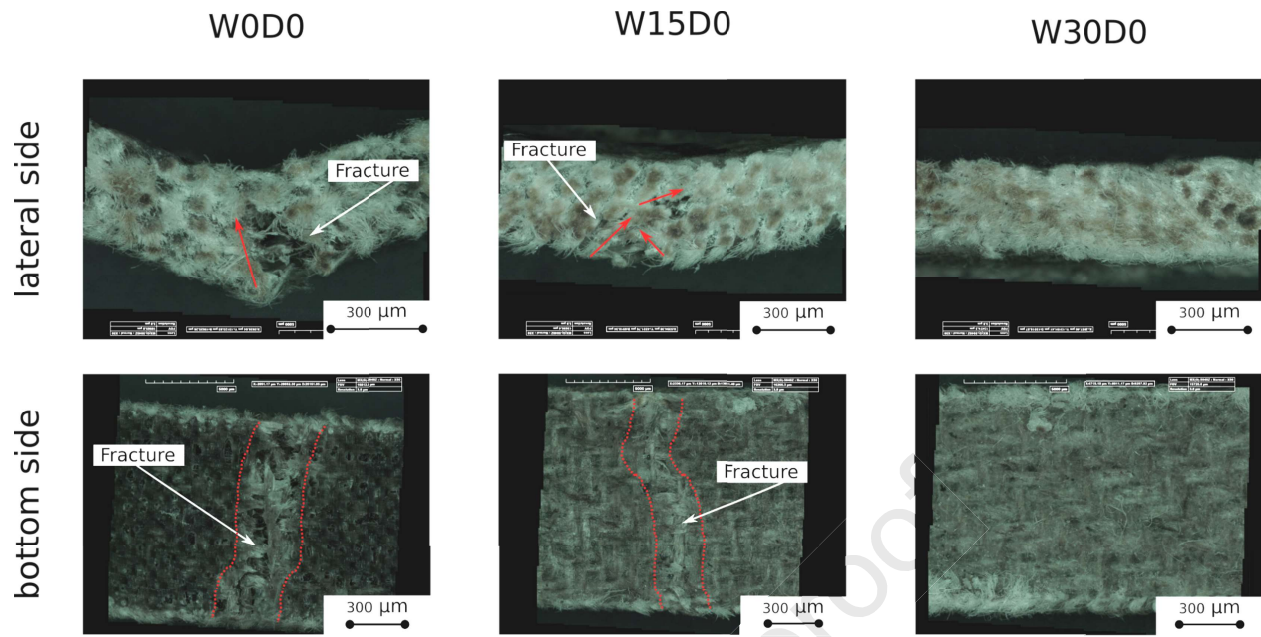
c)

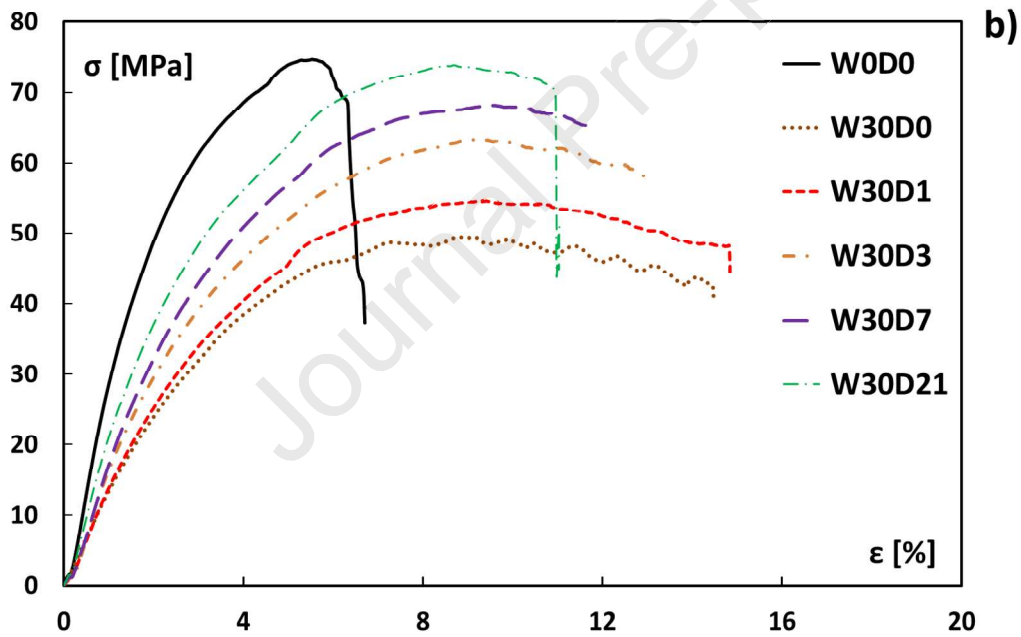
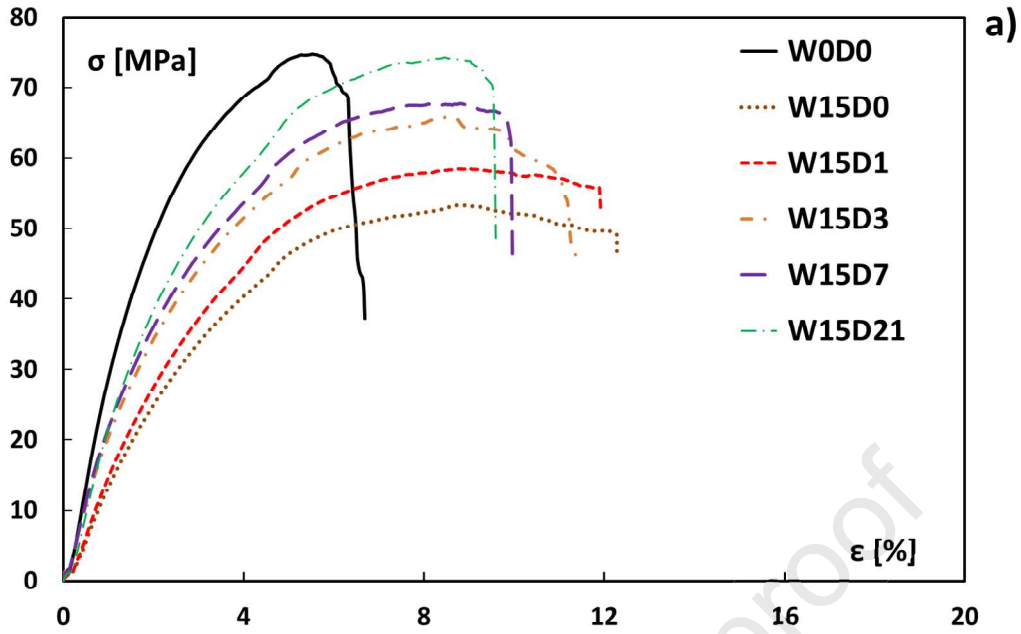


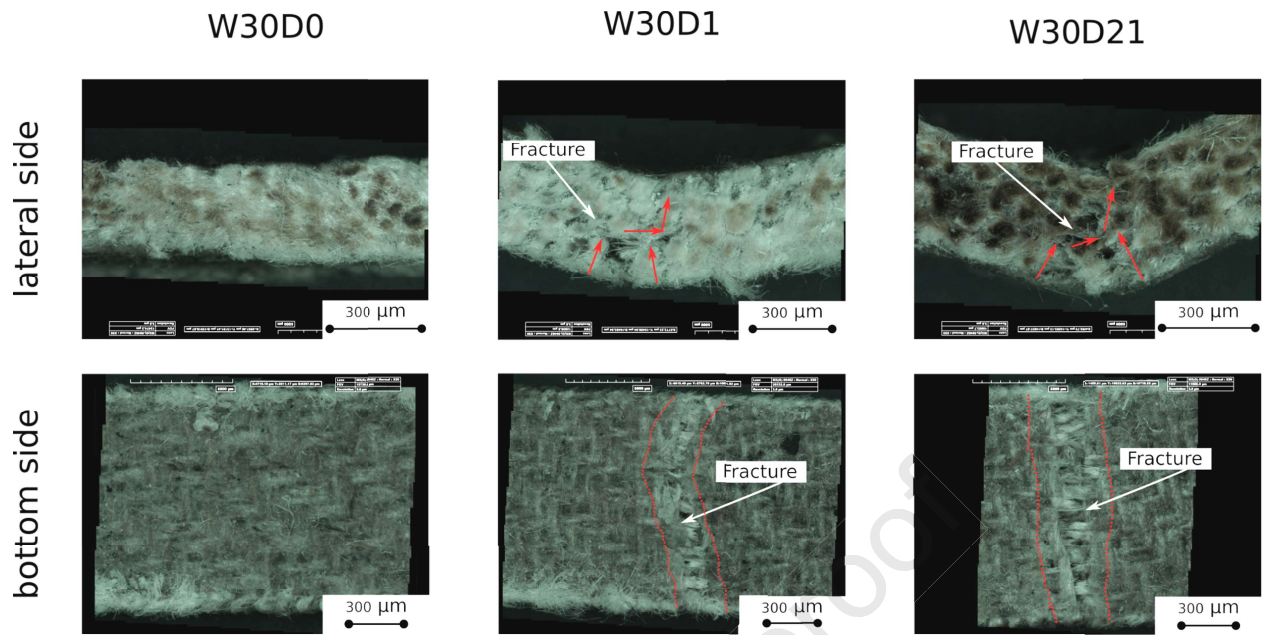
d)











Journal Pre-proof

